



Contents lists available at ScienceDirect

Combustion and Flame

journal homepage: www.elsevier.com/locate/combustflame

Kinetic effects of non-equilibrium plasma-assisted methane oxidation on diffusion flame extinction limits

Wenting Sun^a, Mruthunjaya Uddi^a, Sang Hee Won^a, Timothy Ombrello^b, Campbell Carter^b, Yiguang Ju^{a,*}

^a Department of Mechanical and Aerospace Engineering, Princeton University, Princeton, NJ 08544, USA

^b US Air Force Research Laboratory, Propulsion Directorate, Wright-Patterson AFB, OH 45433, USA

ARTICLE INFO

Article history:

Received 25 March 2011
 Received in revised form 13 June 2011
 Accepted 18 July 2011
 Available online xxx

Keywords:

Plasma assisted combustion
 Nanosecond pulsed discharge
 Plasma flame chemistry reactions
 Path flux analysis
 Counterflow extinction
 Partially premixed flames

ABSTRACT

The kinetic effects of low temperature non-equilibrium plasma assisted CH₄ oxidation on the extinction of partially premixed methane flames was studied at 60 Torr by blending 2% CH₄ by volume into the oxidizer stream of a counterflow system. The experiments showed that non-equilibrium plasma can dramatically accelerate the CH₄ oxidation at low temperature. The rapid CH₄ oxidation via plasma assisted combustion resulted in fast chemical heat release and extended the extinction limits significantly. Furthermore, experimental results showed that partial fuel mixing in the oxidizer stream led to a dramatic decrease of O concentration due to its rapid consumption by CH₄ oxidation at low temperature. The products of plasma assisted CH₄ oxidation were measured using the Two-photon Absorption Laser-Induced Fluorescence (TALIF) method (for atomic oxygen, O), Fourier Transform Infrared (FTIR) spectroscopy, and Gas Chromatography (GC). The product concentrations were used to validate the plasma assisted combustion kinetic model. The comparisons showed the kinetic model over-predicted the CO, H₂O and H₂ concentrations and under-predicted CO₂ concentration. A path flux analysis showed that O generated by the plasma was the critical species for extinction enhancement. In addition, the results showed that O was produced mainly by direct electron impact dissociation reactions and the collisional dissociation reactions of electronically excited molecules with O₂. Moreover, these reactions involving electron impact and excited species collisional dissociation of CH₄ contributed approximately a mole fraction of 0.1 of total radical production. The present experiments produced quantitative species and extinction data of low temperature plasma assisted combustion to constrain the uncertainties in plasma/flame kinetic models.

© 2011 The Combustion Institute. Published by Elsevier Inc. All rights reserved.

1. Introduction

Recently, plasma assisted combustion has drawn attention for its potential to enhance combustion performance in gas turbines, scramjets, and internal combustion engines. Furthermore, extensive efforts have been made to understand the kinetic processes in plasma–flame interactions [1–17]. However, plasma assisted combustion involves strong coupling effects not only from the flow and heat interaction but also from the simultaneous production of active radicals, excited species, ions/electrons, and other intermediate species. Consequently, one of the major challenges is to decouple the complex plasma–flame interactions so that the kinetic contribution of individual species produced by plasma can be understood at the elementary reaction level [15,16]. As such, it is of great importance to (i) develop well-defined plasma-

combustion systems that can provide quantitative, fundamental experimental data to understand the effects of plasma generated species and (ii) develop and validate plasma-assisted combustion kinetic mechanisms.

Many experimental studies have been carried out to understand the role of plasma generated species on ignition, flame speed, and flame stabilization. For ignition studies, the reduction of ignition delay time by non-equilibrium nanosecond pulsed discharges was reported in Refs. [11,18]. The results showed that the ignition delay times could be reduced by about an order of magnitude with the action of plasma. An increase of atomic oxygen (O) concentration was observed with plasma and explained as a major factor for the decrease of ignition delay times. Recently, a major kinetic pathway of O production with plasma has been revealed through the quantitative measurements of O and excited N₂ concentrations [8,19], which has advanced the current understanding of plasma assisted combustion at the elementary reaction level.

The efforts on quantitative understanding of the enhancement mechanism through the flame/plasma interaction has been made

* Corresponding author. Fax: +1 609 258 6233.

E-mail address: yju@princeton.edu (Y. Ju).

Report Documentation Page

Form Approved
OMB No. 0704-0188

Public reporting burden for the collection of information is estimated to average 1 hour per response, including the time for reviewing instructions, searching existing data sources, gathering and maintaining the data needed, and completing and reviewing the collection of information. Send comments regarding this burden estimate or any other aspect of this collection of information, including suggestions for reducing this burden, to Washington Headquarters Services, Directorate for Information Operations and Reports, 1215 Jefferson Davis Highway, Suite 1204, Arlington VA 22202-4302. Respondents should be aware that notwithstanding any other provision of law, no person shall be subject to a penalty for failing to comply with a collection of information if it does not display a currently valid OMB control number.

1. REPORT DATE 2011	2. REPORT TYPE	3. DATES COVERED 00-00-2011 to 00-00-2011
4. TITLE AND SUBTITLE Kinetic effects of non-equilibrium plasma-assisted methane oxidation on diffusion flame extinction limits	5a. CONTRACT NUMBER	
	5b. GRANT NUMBER	
	5c. PROGRAM ELEMENT NUMBER	
6. AUTHOR(S)	5d. PROJECT NUMBER	
	5e. TASK NUMBER	
	5f. WORK UNIT NUMBER	
7. PERFORMING ORGANIZATION NAME(S) AND ADDRESS(ES) Princeton University, Department of Mechanical and Aerospace Engineering, Princeton, NJ, 08544	8. PERFORMING ORGANIZATION REPORT NUMBER	
9. SPONSORING/MONITORING AGENCY NAME(S) AND ADDRESS(ES)	10. SPONSOR/MONITOR'S ACRONYM(S)	
	11. SPONSOR/MONITOR'S REPORT NUMBER(S)	
12. DISTRIBUTION/AVAILABILITY STATEMENT Approved for public release; distribution unlimited		
13. SUPPLEMENTARY NOTES		
14. ABSTRACT The kinetic effects of low temperature non-equilibrium plasma assisted CH₄ oxidation on the extinction of partially premixed methane flames was studied at 60 Torr by blending 2% CH₄ by volume into the oxidizer stream of a counterflow system. The experiments showed that non-equilibrium plasma can dramatically accelerate the CH₄ oxidation at low temperature. The rapid CH₄ oxidation via plasma assisted combustion resulted in fast chemical heat release and extended the extinction limits significantly. Furthermore experimental results showed that partial fuel mixing in the oxidizer stream led to a dramatic decrease of O concentration due to its rapid consumption by CH₄ oxidation at low temperature. The products of plasma assisted CH₄ oxidation were measured using the Two-photon Absorption Laser-Induced Fluorescence (TALIF) method (for atomic oxygen, O), Fourier Transform Infrared (FTIR) spectroscopy and Gas Chromatography (GC). The product concentrations were used to validate the plasma assisted combustion kinetic model. The comparisons showed the kinetic model over-predicted the CO, H₂O and H₂ concentrations and under-predicted CO₂ concentration. A path flux analysis showed that O generated by the plasma was the critical species for extinction enhancement. In addition, the results showed that O was produced mainly by direct electron impact dissociation reactions and the collisional dissociation reactions of electronically excited molecules with O₂. Moreover, these reactions involving electron impact and excited species collisional dissociation of CH₄ contributed approximately a mole fraction of 0.1 of total radical production. The present experiments produced quantitative species and extinction data of low temperature plasma assisted combustion to constrain the uncertainties in plasma/flame kinetic models.		
15. SUBJECT TERMS		

16. SECURITY CLASSIFICATION OF:			17. LIMITATION OF ABSTRACT Same as Report (SAR)	18. NUMBER OF PAGES 9	19a. NAME OF RESPONSIBLE PERSON
a. REPORT unclassified	b. ABSTRACT unclassified	c. THIS PAGE unclassified			

Standard Form 298 (Rev. 8-98)
Prescribed by ANSI Std Z39-18

by several research groups [12,15,16,20]. Ombrello and co-workers have demonstrated experimentally how to isolate singlet oxygen ($O_2(a^1\Delta_g)$) and ozone (O_3) from other plasma related species and shown that both (at concentrations of several thousand ppm) can enhance flame speeds by a few percent [15,16]. The experimental data further revealed that the current kinetic model for $O_2(a^1\Delta_g)$ significantly over-predicted the enhancement for hydrocarbon flames, due to the lack of understanding of collisional quenching rates of $O_2(a^1\Delta_g)$ with hydrocarbon species. Enhancement of flame stability by a non-equilibrium plasma discharge or an electric field in partially premixed systems also have been observed for lifted flames [13,14,21]. Additionally, different explanations for plasma assisted combustion have been given, based on the production of H_2 and CO [13], the formation of active radicals such as OH and O [14], as well as the ionic wind [21]. Unfortunately, in spite of rigorous experimental investigations, the kinetic contribution from the plasma/flame interaction has not been fully characterized due to the complexity of either their interaction or the experiment itself.

Recently, a nanosecond pulsed discharge system has been integrated into the oxidizer side of a counterflow flame configuration, in order to obtain a simplified plasma/flame interaction [17]. The experimental results revealed that the extinction limit of diffusion flames can be significantly extended by applying the discharge on the oxidizer side to produce O . However, considering a practical application, where the flow condition is controlled by the intensive turbulent mixing, partial/full oxidation of the premixture with plasma would be one of the important factors that dominate the flame/plasma interactions. In this case, it is important to investigate how the chemical reactivity of the premixture can be induced or promoted through the plasma/flame interactions, particularly in the low temperature regime (<1000 K). Moreover, due to a dearth of quantitative data, the current plasma combustion kinetic mechanism for ignition [8] remains untested for low temperature CH_4 oxidation. Consequently, it is essential to provide quantitative measurements of species not only to validate of current kinetic models but also to advance the fundamental understanding of kinetic aspects of plasma/flame interactions.

Accordingly, the goal of the present study was to investigate the effect of plasma assisted CH_4 oxidation at the low temperature regime on the extinction limits of diffusion flames with partially premixed oxidizer in the counterflow configuration. The species concentrations have been measured with TALIF for O and Fourier Transform Infrared (FTIR) spectroscopy and Gas Chromatography (GC) for stable intermediate species in order to characterize the performance of nanosecond pulsed discharge in a partially premixed oxidizer stream and to validate the current plasma-combustion kinetic model. This model has been validated further against the experimental measurements of extinction limits. Path flux analyses have also been conducted to identify and understand the important CH_4 oxidation pathways in plasma assisted combustion.

2. Experimental methods and kinetic modeling

2.1. Partially premixed counterflow flame system with nano-second pulsed discharge

A schematic of the experimental system is shown in Fig. 1. The setup consisted of a pair of counterflow burners that were located in a low pressure chamber with a volume of 81 L. The inner diameters of the reactant and co-flow nozzles were 20 and 28 mm, respectively. The burner separation distance of the opposed nozzles were maintained to be equal to the nozzle diameter, 20 mm, to avoid the perturbation of the boundary condition from

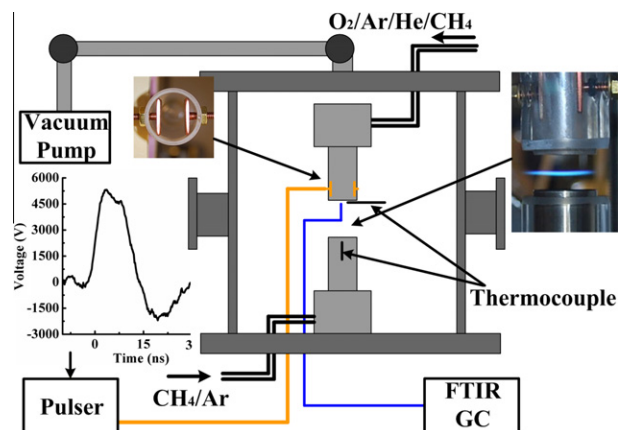


Fig. 1. Schematic of experimental setup.

thermal expansion. The co-flowing inert (Ar) curtain provided the isolation of the flame from the environment and burner cooling as well. A honeycomb plate was placed inside the reactant nozzles to ensure that the flow field was uniform. The counterflow nozzles were made of quartz, and two parallel bare metal electrodes (a copper alloy that is corrosion resistant to avoid the catalytic effect of copper) were located inside the tubes of the upper nozzle. The electrodes were $15\text{ mm} \times 22\text{ mm} \times 1\text{ mm}$ (thick) and were separated by 10 mm (inset in Fig. 1). The electrode edges were smoothed to avoid the local concentration of electric field and dielectric breakdown. The front ends of the electrodes were 10 mm away from the exit to avoid electrical interaction with the thermocouples. The experimental pressure was 60 Torr, the diffusion time scale (approximately 1 ms, estimated by l^2/D , where l was the electrode thickness, and D the diffusivity ($\sim 10^{-3}\text{ m}^2/\text{s}$) of O_2 at 300 K and 60 Torr) was much shorter than the flow residence time (approximately 10 ms). Thus, the diffusion was sufficiently fast, and the effect of the electrodes on the flow field inside the tube was negligible. To ensure that the stagnation plane was formed in the middle of the two burner exits, the momenta of the two reactant streams were matched. During the experiments, He and Ar were used as dilution gases for the partially premixed oxidizer stream (He can improve the uniformity of the discharge [22], but it was difficult to maintain the flame if He was used as the only dilution gas due to the large thermal diffusivity at low pressure. Thus in our experiments, a He and Ar mixture was used as the diluent). The composition of the oxidizer stream was fixed at $O_2/Ar/He/CH_4$ (0.26:0.32:0.4:0.02) to observe the effect of CH_4 doping in the oxidizer. The fuel stream was CH_4 diluted by Ar (fuel mole fraction varied from 0.2 to 0.4). A nanosecond pulse generator (FID FPG 30-50MC4) was used to generate the non-equilibrium plasma to activate the partially premixed oxidizer stream. The pulse generator is capable of producing repetitive 32 kV pulses with pulse duration of 12 ns, full width at half maximum (FWHM). The frequency of the pulse generator is adjustable from 1 to 50 kHz. A typical voltage waveform measured by a LeCroy high voltage probe (PPE20KV), is embedded in Fig. 1. The current through the electrodes was measured with a Pearson Coil (Model 6585). The pulse energy supplied to the discharge was estimated from the time integration of the voltage and current profiles and found to be approximately 1.27 mJ/pulse. The characteristics of voltage-current were independent of pulse repetition frequency. Therefore, average powers were calculated to be 5.1, 12.7, 25.4, 38.1 and 50.8 W at the respective frequencies of 4, 10, 20, 30 and 40 kHz. The amplitude of the voltage was fixed at 5.3 kV for all tested experimental conditions, as shown in Fig. 1. The direct image of the nanosecond repetitive discharge is shown in Fig. 2a at

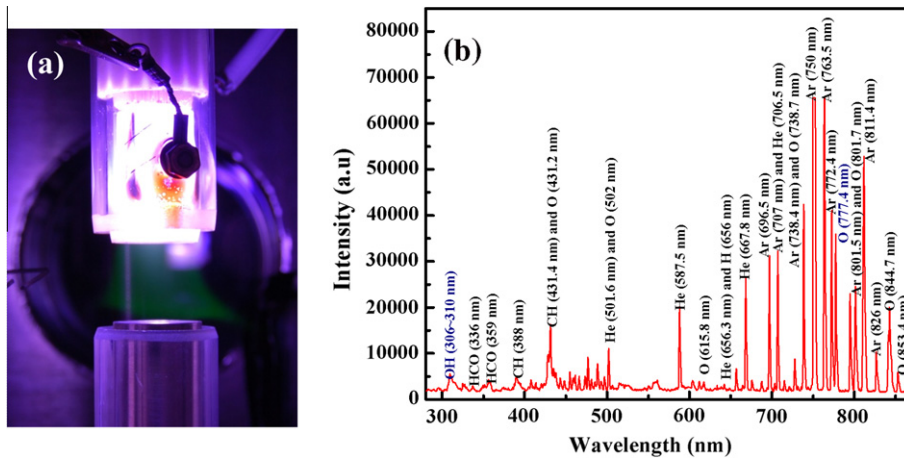


Fig. 2. Discharge at Ar/He/O₂/CH₄ (0.32/0.4/0.26/0.02 by volume), $d = 20$ mm, $f = 30$ kHz, $P = 60$ Torr, (a) direct image, (b) optical emission spectrum.

a pulse repetition frequency of 30 kHz. The optical emission spectrum of the discharge is shown in Fig. 2b. Figure 2b shows strong emissions from excited O, OH, HCO, CH, He, and Ar, which indicated the radical formation from CH₄ oxidation during the discharge. It was also observed that the strongest emissions were from excited Ar and O (750 nm and 777.4 nm, respectively) and the intensity of all emission lines increased with the increase of pulse repetition frequency. Thus, the plasma assisted CH₄ oxidation was presumed to be affected by the pulse repetition frequency, and the excited Ar and O may play an important role in the CH₄ oxidation. The intensity of excited He emission was not strong, however; this is because the excitation energy of He is relatively high (19.8 eV) compared to that of Ar (11.5 eV). Detailed discussions of the kinetic process will be given in the next section.

The extinction strain rates were measured by fixing the fuel mole fraction and increasing the flow velocity gradually until extinction occurred. At the same time, temperatures at the burner exits were measured simultaneously using thermocouples. One thermocouple (380 μ m bead diameter) was fixed at the exit of the lower fuel nozzle, and another movable thermocouple was used to monitor the temperature at the exit of the upper nozzle. The movable thermocouple was coated with MgO and covered with a grounded Nickel-Chrome sheath (with 1 mm outer diameter) to remove the electromagnetic interference from the discharge.

The major products (CH₄, CO, CO₂, CH₂O, and H₂O) from the plasma assisted CH₄ oxidation in the oxidizer stream were measured by using an FTIR spectrometer (Nicolet Magna-IR 550). A quartz probe with an inlet diameter 1 mm was placed axially at the oxidizer side nozzle exit and was attached to a heated line (to avoid H₂O condensation) of the FTIR spectrometer. The pressure and temperature in the FTIR system were held constant at 31 Torr and 393 K, respectively. For H₂ measurement, a micro GC system (INFICON 3000) was used. The calibrations were performed by flowing sample gas with known species concentrations through the FTIR or GC at conditions identical to those of the experiments. The relative mole fraction uncertainties of sampling measurements were found to be less than $\pm 1\%$ for CH₄, CO, CO₂ and $\pm 5\%$ for H₂O and H₂. The uncertainty of the CH₂O measurement was ± 80 ppm. The sampling was also performed by using a quartz probe with 6 mm diameter. The results were identical with that of 1 mm diameter probe which indicated the uniformity of the properties of the counterflow system in the center region and the validity of one dimensional approximation.

2.2. Two-photon Absorption Laser Induced Fluorescence (TALIF) system

The TALIF method, calibrated with Xenon, was used to measure the absolute O concentration at the oxidizer-side nozzle exit. The TALIF system used in this study was described in detail in our previous study [17], and thus only a summary of this method is presented here. Ground state O is excited by absorbing two photons at a wavelength of 225.7 nm. The transition between the excited $3p^3P$ state and the $3s^3S$ state will release a single photon at 844.6 nm. Xenon can be excited from $5p^6^1S_0$ to $6p^1[3/2]2$ with the two photons at 224.31 nm; de-excitation to $6s^1[1/2]1$ corresponds to fluorescence at 834.91 nm. The number density of O (N_O) was calculated using the following equation in terms of the known number density of Xenon (N_{Xe}) [8],

$$N_O = \frac{S_O}{S_{Xe}} g_{ND} \frac{a_{21}(Xe)}{a_{21}(O)} \left(\frac{\sigma^{(2)}(Xe)}{\sigma^{(2)}(O)} \right) \left(\frac{v_O}{v_{Xe}} \right)^2 \times \frac{1}{F_O(T)} N_{Xe}$$

where S_O and S_{Xe} are the observed fluorescence signals for O and Xenon, respectively, $a_{21} = \frac{A_{21}}{A_{21}+Q}$ the fluorescence quantum yields (A_{21} and Q are spontaneous emission and quenching rates, respectively), $\sigma^{(2)}$ the two photon absorption cross sections of Xe and O, $F_O(T)$ the atomic oxygen Boltzmann factor for the lower level of the two photon absorption, v_i the photon energies, and g_{ND} the neutral density filter factor (1.82×10^{-3} from manufacturer). These values can be found or easily calculated based on the data in Refs. [8,23].

An Nd:YAG laser was used to generate 532 nm to pump a tunable dye laser operating at ~ 573 nm. This 573 nm beam was frequency doubled and mixed with the 1064 nm beam of the Nd:YAG laser to get a ~ 226 nm beam of ~ 10 μ J/pulse required for the TALIF diagnostics. The TALIF signal was observed using an 850 nm bandpass filter of 40 nm FWHM and a Hamamatsu photomultiplier (R636-10). A separate vacuum cell was used to obtain the Xenon atom two-photon fluorescence spectrum. Corrections for the transmission of the vacuum cell and bandpass filter were made to find the O density by the method described in Refs. [8,23]. The overall relative mole fraction uncertainty of the TALIF measurement was approximately $\pm 40\%$.

2.3. Computational approach with plasma-combustion kinetic model

The kinetic model used in this work was an integration of the air plasma model [8] together with USC Mech II [24]. In addition,

in order to consider species dissociation by excited Ar and He and dissociation of CH₄ by electron impact, additional elementary reactions involving the dilution gases (He/Ar) and CH₄ were added (Table 1). The plasma combustion model incorporates a set of species conservation equations for number densities of neutral, charged, and excited species produced in the plasma, O, O₂, O₃, e, O₂⁺, O⁺, O⁻, O₂⁻, O₂(a¹Δ_g), O₂(b¹Σ), O(¹D), Ar(+), Ar(3p⁵(²P_{3/2})4s), Ar(3p⁵(²P_{1/2})4s), Ar(3p⁵(²P_{3/2})4p) (Ar* for simplicity, with respective excitation energies of 11.5, 11.7, and 12.9 eV), He(+), He(2s³S), He(2s¹S), He(2p³P), He(2p¹P), He(3s¹S), and He(4p¹P) (He* for simplicity, with respective excitation energies of 19.8, 20.6, 21, 21.2, 22.9, and 23.7 eV), as well as the energy conservation

Table 1
List of Ar/He/CH₄ related reactions involved in Ar/He/O₂/CH₄ mixture discharge.

Reaction	Rate (cm ³ s ⁻¹)	References
e + CH ₄ = e + CH ₃ + H	σ ^a	[27]
e + CH ₄ = e + CH ₄ (+)	σ	[28]
e + CH ₄ (+) = CH ₂ + 2H	1.7 × 10 ⁻⁷ (300/T) ^{0.5}	[28]
e + CH ₄ (+) = CH ₃ + H	1.7 × 10 ⁻⁷ (300/T) ^{0.5}	[28]
CH ₄ (+) + O ₂ = CH ₄ + O ₂ (+)	5 × 10 ⁻¹⁰	[28]
Ar + e = Ar ⁺ + e	σ	[28]
Ar + e = Ar(+)+ 2e	σ	[28]
Ar ⁺ + O ₂ = Ar + 2O	2 × 10 ⁻¹⁰	[28]
Ar(+)+ O ₂ = Ar + O ₂ (+)	1 × 10 ⁻¹⁰	[28]
Ar ⁺ + CH ₄ = Ar + CH ₂ + 2H	3.3 × 10 ⁻¹⁰	[28]
Ar ⁺ + CH ₄ = Ar + CH + H ₂ + H	5.8 × 10 ⁻¹⁰	[28]
Ar ⁺ + CH ₄ = Ar + CH ₃ + H	5.8 × 10 ⁻¹⁰	[28]
Ar ⁺ + CH ₄ = Ar + CH ₂ + H ₂	5.8 × 10 ⁻¹⁰	[28]
Ar(+)+ CH ₄ = Ar + CH ₃ (+)+ H	6.5 × 10 ⁻¹⁰	[28]
Ar(+)+ CH ₄ = Ar + CH ₂ (+)+ H ₂	1.4 × 10 ⁻¹⁰	[28]
He + e = He ⁺ + e	σ	[29]
He + e = He(+)+ 2e	σ	[29]
He ⁺ + O ₂ = He + O ₂ (+)+ e	1.5 × 10 ⁻¹¹ T ^{0.5}	[29]
He ⁺ + O = He + O(+)+ e	1.5 × 10 ⁻¹¹ T ^{0.5}	[29]
He(+)+ O ₂ = He + O(+)+ O	0.6 × 10 ⁻¹¹ T ^{0.5}	[29]
He(+)+ O ₃ = He + O ₂ + O(+)	0.6 × 10 ⁻¹¹ T ^{0.5}	[29]
He(+)+ O ₂ (a ¹ Δ _g) = He + O(+)+ O	0.6 × 10 ⁻¹¹ T ^{0.5}	[29]
He(+)+ O(¹ D) = He + O(+)	2.9 × 10 ⁻¹² T ^{0.5}	[29]
He + 2O = He ⁺ + O ₂	1 × 10 ⁻³³	[29]
He + O(¹ D) = He + O	1 × 10 ⁻¹⁰	[30]
He ⁺ + CH ₄ = He + CH + H ₂ + H	5.6 × 10 ⁻¹³	[31]

^a The rate is calculated by the Boltzmann solver using experimentally measured cross-sections, σ.

equation for prediction of the temperature of the mixture. This set of equations are coupled with the steady state, two-term expansion Boltzmann equation for the electron energy distribution function (EEDF) of the plasma electrons using experimentally measured cross sections of electron impact electronic excitation, dissociation, ionization, and dissociative attachment processes. The Boltzmann equation calculates the rate coefficients of the electron impact elementary reactions by averaging the cross sections over the EEDF. The kinetic model also incorporates chemical reactions of excited electronic species, electron–ion recombination and ion–ion neutralization processes, ion–molecule reactions, and electron attachment and detachment processes. Note that the present model does not solve the Poisson equation for the electric field and therefore does not take into account charge separation and sheath formation near the electrode. So in the present work, the reduced electrical field (*E/N* ratio) in the plasma was considered to be an adjustable parameter, varied until the CH₄ concentration (at the nozzle exit, 1 cm away from the end of the discharge region) matched with the experimental results at the burner exit. CH₄ concentration was used here to determine the *E/N* ratio because CH₄ concentration measurement had the smallest uncertainty (1% vs. 40% for TALIF of O). Therefore, only the concentrations of CO, CO₂, H₂O, H₂, CH₂O, and O from the simulations were compared with the experiments. The model was also employed to calculate the radical/atom (OH and H) concentrations by matching the O concentrations from the simulations with the corresponding experimental values. The radical concentrations were further used as the boundary conditions for extinction limit calculations in Section 3.2. More details about this model can be found at Refs. [25,26].

3. Results and discussion

3.1. Effects of discharge repetition rate on species concentrations from plasma assisted CH₄ oxidation

FTIR and GC instrumentation were used to quantify the major stable products of the low temperature plasma assisted CH₄ oxidation by sampling at the center of the nozzle exit in the oxidizer stream using quartz probe. Typical FTIR absorption spectra are shown in Fig. 3a–f. Figure 3a shows the FTIR absorption spectra

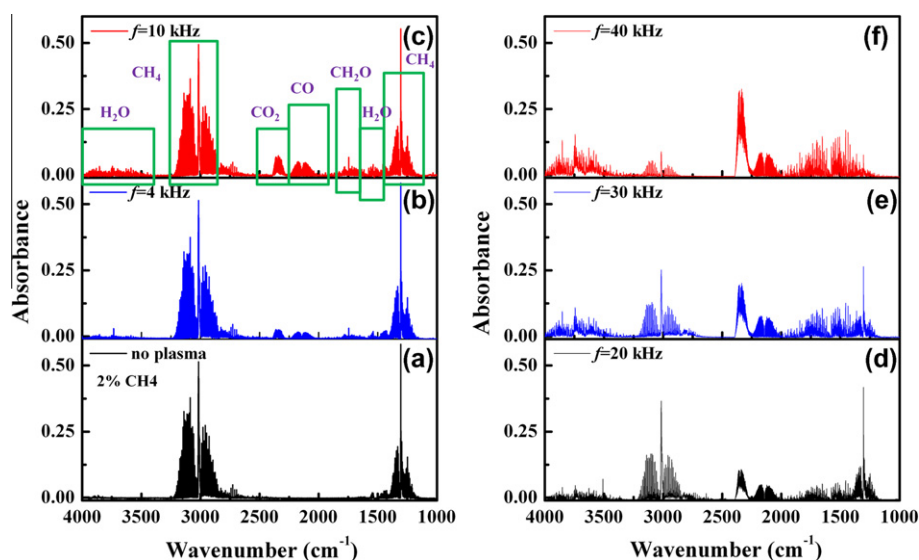


Fig. 3. FTIR spectrum with different pulse repetition frequencies at Ar/He/O₂/CH₄ (0.32/0.4/0.26/0.02 by volume), *P* = 60 Torr; (a) no plasma, (b) *f* = 4 kHz, (c) *f* = 10 kHz, (d) *f* = 20 kHz, (e) *f* = 30 kHz, and (f) *f* = 40 kHz.

without the discharge. The CH_4 absorbance spectrum is seen clearly and shows no effects of any CO_2 and H_2O entrainment from the environment. With the presence of the plasma discharge, the absorbance spectra of CO , CO_2 , H_2O and CH_2O appeared due to the plasma assisted CH_4 oxidation. Moreover, as shown in Fig. 3b–f, with the increase of discharge pulse repetition frequency (or equivalently, discharge power), the concentrations of CO , CO_2 and H_2O increased significantly, and at the same time, the concentration of CH_4 decreased. The dependence of the measured concentrations of CO , CO_2 , H_2 , H_2O , and CH_2O on the plasma pulse repetition rate is shown in Figs. 4–6. In order to validate the plasma flame model, the predicted species concentrations are also plotted in Figs. 5 and 6. In all the FTIR measurements, it was confirmed that the carbon closure with the measured species was 95%, demonstrating that the measurements captured the major carbon containing species in the plasma assisted CH_4 oxidation. It was also observed that carbon black deposited on the electrodes and sampling quartz probe during the experiments and that the minor carbon loss was caused by the formation of carbon black in the plasma discharge. As shown in Figs. 4 and 5, with the increase of pulse repetition frequency, the CH_4 concentration decreased significantly, and nearly a mole fraction of 0.9 of CH_4 was oxidized at pulse repetition frequency $f = 40$ kHz. At the same time, the concentrations of CO , CO_2 and H_2O increased monotonically with f . With the increase of CH_4 oxidation ratio, the oxidizer temperature at the nozzle exit also increased significantly (423 ± 3 K, 613 ± 5 K, 743 ± 5 K, 843 ± 5 K and 933 ± 8 K at $f = 4$ kHz, 10 kHz, 20 kHz, 30 kHz, and 40 kHz, respectively). Note that the concentration of H_2 after low

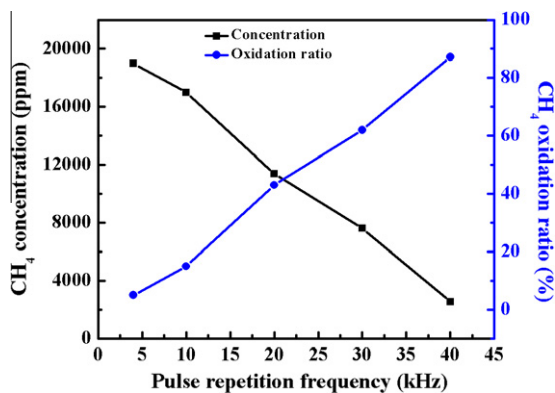


Fig. 4. Dependence of CH_4 concentrations and oxidization ratios on pulse repetition frequency.

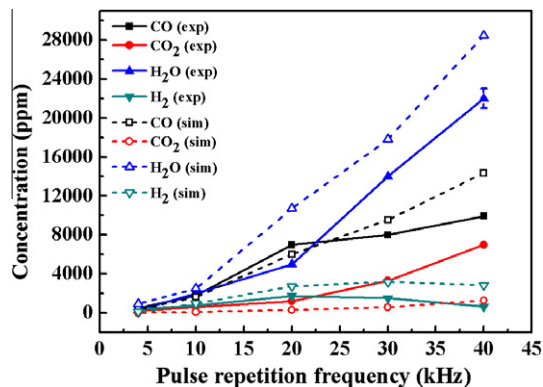


Fig. 5. Dependence of species concentrations at the burner exit on pulse repetition frequency (experiments: solid symbol and solid line; simulations: open symbol and dashed line).

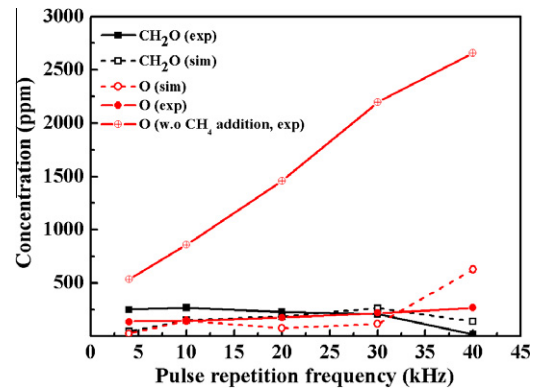


Fig. 6. Dependence of species concentrations at the burner exit on pulse repetition frequency (experiments: solid symbol and solid line; simulations: open symbol and dashed line).

temperature plasma assisted CH_4 oxidation remained very low (less than 2000 ppm). The peak concentration of H_2 occurred at a pulse repetition frequency $f = 20$ kHz. The low value of peak H_2 concentration compared to H_2O concentration suggests that the plasma assisted combustion was not dominated by fuel reforming into H_2 and CO , as will be discussed later. A low peak concentration for CH_2O at $f = 10$ kHz was also observed during the experiments, as shown in Fig. 6. It is shown in both Figs. 5 and 6 that the model captured the correct trend of the relationship between the species concentrations and pulse repetition frequency, but the kinetic model over-predicted CO (up to 44%), CH_2O (up to a factor of 6) and H_2 (up to a factor of 3), and under-predicted CO_2 (up to 89%) by volume, indicating that the model underestimated the overall reactivity in the oxidizer stream.

In order to identify the important CH_4 oxidation pathways and understand the kinetic processes in the plasma assisted CH_4 oxidation mechanism, path flux analysis was performed for a pulse repetition frequency $f = 40$ kHz, and the results are shown in Fig. 7. Methane was dissociated to CH_3 mainly by H abstraction with OH, O and H produced via the plasma discharge. Methane also decomposed to CH_3 , CH_2 and CH via collisions with an electron, Ar^+ and Ar^* (reactions (1)–(6)). The formed CH_3 , CH_2 and CH were oxidized further to CH_2O , HCO , CO and finally CO_2 as shown in Fig. 7a. Among those reaction paths, a total of a mole fraction of 0.12 of CH_4 was decomposed by collisions with electrons, Ar^+ and Ar^* . Molecular hydrogen is another important product of plasma assisted CH_4 oxidation because it can affect greatly the ignition and extinction processes via its fast oxidation chemistry. The reaction path of H_2 is shown in Fig. 7b. The dominant formation path of H_2 was through H abstraction reactions with CH_4 , CH_2O , HO_2 , HCO , CH_2 and CH_3 . The formation of H_2 via $\text{H} + \text{HO}_2 = \text{H}_2 + \text{O}_2$ clearly indicates the nature of low temperature chemistry. This reaction plays an important role at low temperature and high pressure when HO_2 concentration is high [32]. Another formation path of H_2 was through CH_4 decomposition by Ar^* , but only 1.2% of H_2 was formed through this reaction path. Moreover, the concentration of H_2 increased at low pulse repetition frequency, due to the increased H abstraction reaction by H radicals; at high frequency, H_2 concentration then decreased via increased reactivity at higher temperature. Therefore, the concentration of H is important to determining the concentration of H_2 . The reaction paths of H and O are also shown in Fig. 8a and b. Only 11.7% of H was formed via the decomposition of CH_4 by electron impact and excited species collisions through reactions (R1), (R2), (R3), (R4), (R5). The major contribution to H formation was from reaction $\text{CH}_3 + \text{O} = \text{CH}_2\text{O} + \text{H}$. Thus, O concentration is crucial to determining H concentration.

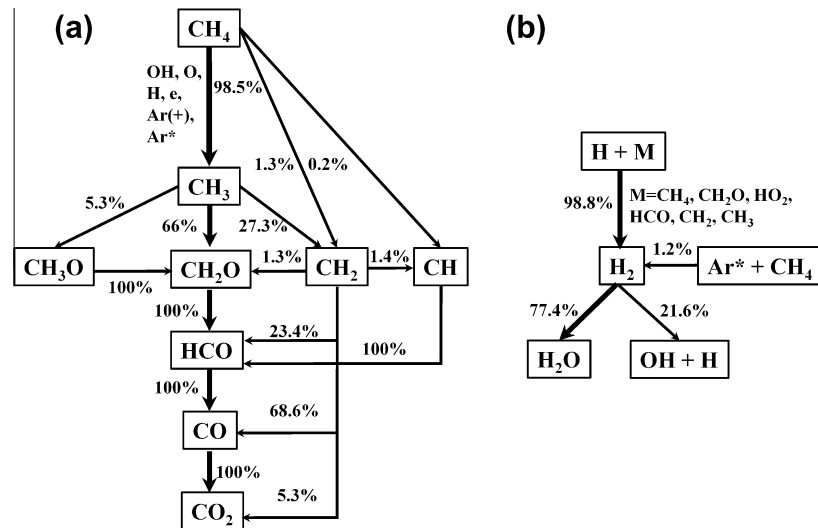


Fig. 7. Reaction paths flux analysis for (a) CH₄ and (b) H₂ at $f = 40$ kHz.

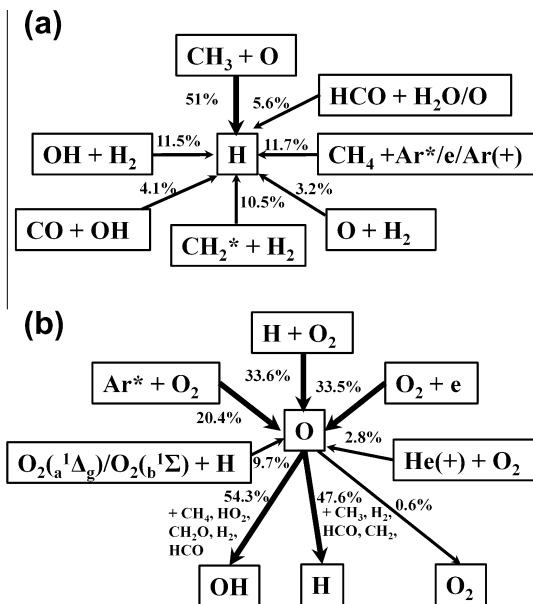
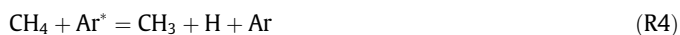
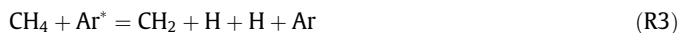


Fig. 8. Reaction paths flux analysis for (a) H and (b) O at $f = 40$ kHz.



The reaction path of O is shown in Fig. 8b. Approximately 54% of O was formed through collisions between O₂ and electrons/Ar^{*}. Among all the three major O production paths, 33.5% was from direct electron impact dissociation of O₂, 20.4% from O₂ collisions with Ar^{*}, and 33.6% from the H + O₂ = OH + O branching reaction. Note from Fig. 8a that the initial H radicals for the branching reac-

tion are formed from the reaction of O with CH₃, which is itself produced by the direct plasma discharge in the partially premixed CH₄/O₂ stream. Therefore, it can be concluded that O production by plasma is the major source to initiate the low temperature plasma assisted CH₄ oxidation. Moreover, the partial CH₄/O₂ premixing increases H production and accelerates the chain branching process. Once O is generated by the discharge, it is consumed rapidly by CH₄ and its intermediate oxidized and dissociated products (CH₃, CH₂, CH₂O, HCO, HO₂ and H₂). It is shown in Fig. 8b that the major consumption path of O is to generate OH and H, which are important to the CH₄ oxidation process. OH and H then further react with fuel and its fragments, which become the dominant reaction paths of the fuel decomposition. Only a small amount (0.6%) of O recombines to O₂ (Surface recombination reaction of O was not considered in this study. This was accounted for by measuring the O concentration at the center of the nozzle and comparing with the simulations). Note that the reaction path from O to O₃ is negligible in this study due to the high temperature conditions. Furthermore, the concentrations of reactive oxidant ions (O₂⁺, O⁻) are several orders of magnitude lower than O, and thus their effects are also negligible. This indicates that when the discharge is applied to the premixture of fuel and oxidizer, O can be consumed more efficiently by the fuel and its intermediate oxidation and dissociation products rather than through recombination. Based on the above analysis, it is clear that O production within a plasma discharge in a partially premixed fuel and oxidizer is critical for H₂ and H formation and subsequent CH₄ oxidation. Therefore, in order to predict other species, O formation through the collision-induced O₂ dissociation by electrons and excited species needs to be accurately predicted. In addition, to improve the CH₄ oxidation efficiency (the consumption efficiency of O), the plasma discharge needs to be implemented in a partially premixed lean fuel/oxidizer mixture.

In order to determine the concentration of O and compare with the kinetic model prediction, the Xenon calibrated, Two Photon Absorption Laser Induced Fluorescence (TALIF) method was used. The relationship between O concentration and pulse repetition frequency (for a flow velocity of 200 cm/s) with and without fuel premixing is plotted in Fig. 6. For plasma discharge in a partial premixture of fuel and oxidizer, it is shown that with the increase of pulse repetition frequency, the O concentration increased, but the increase was very low, less than 300 ppm even at $f = 40$ kHz (note that the TALIF detection limit can be as low as several ppm

[8]). The low rate of increase of O production versus f suggests that the cause is rapid CH₄ oxidation at high plasma repetition frequency by the induced chain reactions (shown in Fig. 8b). To demonstrate this fact, the O concentration without fuel premixing was also measured at the same condition. Figure 6 shows that the concentration of O increased sharply from 530 ppm to 2700 ppm when the pulse repetition frequency increased from 4 kHz to 40 kHz. This result confirmed that the increased CH₄ oxidation at high plasma frequency was due to the increased production of O. The simulation results of O and CH₂O concentrations are also shown in Fig. 6, together with the experimental measurements of CH₂O concentration. The calculated concentrations of O and CH₂O intersected with the experimental results, but the deviations became large at $f = 40$ kHz.

As analyzed, the model under-predicted the concentration of CO₂, and over-predicted CO and H₂, which indicated an overall lower reactivity of the mixture. For O and CH₂O prediction, the kinetic model significantly under-predicted their concentrations at low pulse repetition frequency and over-predicted the concentrations at high pulse repetition frequency. This may be due to the missing reaction paths involving peroxide species at low temperature and those involving interactions of excited species with hydrocarbon species and its products. For example, the HO₂ + X (X = H, OH) reaction rates have large uncertainty at low temperature, and the OH + O + M = HO₂ + M reaction, which is not included in the current combustion mechanism, may become important at low temperature [32]. In addition, a fraction of O atoms was excited to O(¹D), which is much more reactive, especially at low temperature conditions. But, unfortunately, reactions involving O(¹D) and hydrocarbon species are not well characterized and are absent in the current kinetic model (except O(¹D) + H₂ = H + OH [33], which is 10⁷ faster than O + H₂ = H + OH at 300 K). The formation of CH₂O was primarily from the reaction CH₃ + O = CH₂O + H. If the concentration of O was over-predicted (or under-predicted), the concentration of CH₂O would also be over-predicted (or under-predicted). Likewise, H₂O can react with O(¹D) via the H₂O + O(¹D) = 2OH reaction and can also be dissociated by electrons and Ar* to generate OH and H. The generation of OH can accelerate the oxidation of CO.

The kinetic model also showed the formation of C₂H₆ (~200 ppm), but the C₂H₆ absorption spectrum was not observed in the FTIR experiments. Previous research in a lean CH₄/air discharge [34] also showed no C₂H₆ formation, and thus the reaction CH₃ + CH₃ = C₂H₆ was over-estimated or the consumption path of C₂H₆ was underestimated at low temperatures. Furthermore, it is known that the current kinetic mechanism has not been validated below 700 K. More quantitative experimental data at low temperature conditions are thus required to improve the predictability of the kinetic mechanism.

3.2. Extinction strain rates measurement and computation

The extinction strain rates of the CH₄/O₂ diffusion flames were measured without and with plasma (at $f = 4, 10, 20, 30,$ and 40 kHz). A definition of global strain rate [35]

$$a_0 = \frac{2U_o}{L} \left(1 + \frac{U_f \sqrt{\rho_f}}{U_o \sqrt{\rho_o}} \right) \quad (1)$$

was adopted and compared with numerical simulations. Here U is the speed of the flow, ρ the density of the flow, and L the gap distance between the two nozzles. The subscripts o and f refer to the oxidizer and fuel side, respectively. The use of global strain rate was found to be appropriate for mechanism validation [36], and the global strain rates were used in this study for both experiments and simulations.

In this experiment, the composition of the partially premixed oxidizer stream was fixed at a volume ratio of 0.02/0.26/0.32/0.4 for CH₄/O₂/Ar/He. The fuel stream was composed of CH₄ and Ar, and the CH₄ mole fractions varied from 0.2 to 0.4. During the measurements, the fuel mole fraction was fixed, and the flow velocity of both sides increased gradually. With the increase of flow velocity, the strain rate increased, and the flame had less residence time to complete the CH₄ oxidation and thus extinguished when the strain rate was above a critical value. This critical strain rate at flame extinction was recorded as the global extinction strain rate. Figure 9 shows the relationship of extinction strain rates and fuel mole fractions without plasma and with plasma at pulse repetition frequencies of $f = 4$ and 10 kHz (with oxidizer temperature $T_o = 423 \pm 4$ K and 613 ± 5 K, the oxidizer side flow rates were among 1.92–2.18 SLPM and 2.22–2.41 SLPM at fuel mole fractions from 0.34 to 0.4, respectively). Extinction strain rates without CH₄ addition (O₂/Ar/He ratio of 0.28/0.32/0.4) were also presented in Fig. 9 as reference. The experiments were compared further with numerical simulations. The simulations were computed using OPP-DIFF of the CHEMKIN package [37] with a modified arc-length continuation method [38] for plug flow. All simulations were performed by setting the boundary conditions using the measured temperatures and species concentrations (using FTIR, GC and TALIF instruments). The concentrations of H and OH were estimated from the simulation by matching the computational and experimental values of O concentrations, as discussed in Section 3.1. It was noticed that the extinction strain rate was sensitive to the CH₄ mole fraction in the oxidizer stream because this determines the heat release rate in the reaction zone. Thus, the failure to update the species concentrations information as the boundary condition may cause approximately 15% larger calculated extinction strain rates in the simulations. The results in Fig. 9 show that with CH₄ addition, the extinction strain rates were extended significantly and the oxidizer temperature after the plasma activation was higher (613 K and 548 K with and without CH₄ addition at $f = 10$ kHz, respectively). It is also shown that with the increase of the pulse repetition frequency, f , there was a significant increase of extinction limit enhancement and the measured extinction strain rates agree well with the computed values. The present results indicate that the plasma generated CH₄ oxidation plays an important role for the extension of flame extinction limit. This is because when the flame approaches extinction, there was not enough residence time for the CH₄ to complete the oxidation reactions to release the chemical heat. However, plasma can dramatically accelerate the CH₄ oxidation to release the chemical energy at low temperature. The prompt chemical heat release extended the extinction limit.

It was noticed that during the plasma assisted CH₄ oxidation process, part of the CH₄ was reformed into H₂ and CO. Molecular

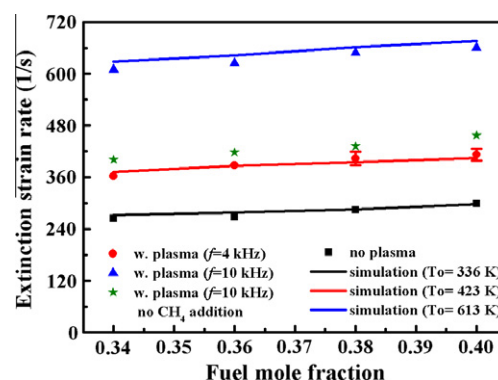


Fig. 9. Dependence of extinction strain rate on fuel mole fraction at the fuel side under different experimental conditions.

hydrogen can extend the extinction limit through its fast chemistry, and previous research [13,20,39] showed that plasma induced fuel reforming, producing a H_2/CO mixture, can enhance the flame stability. Therefore, it is important to examine how the fuel reforming affects the extinction. The present experiment showed that the H_2 formation by non-equilibrium plasma discharge was low. As such, the plasma reforming effect only played a minor role in the extension of the extinction limit. Of course, the H_2 yield depends on the discharge characteristics and fuel concentration in the mixture. It is necessary to understand whether fuel reforming or CH_4 oxidation is more effective in increasing flame stabilization.

Because plasma can cause both CH_4 oxidation and reformation, simulations of the individual effects of plasma assisted CH_4 oxidation and CH_4 reforming were performed and compared in Fig. 10. Here, part of the fuel (CH_4) in the oxidizer stream was assumed to be ideally oxidized to H_2O and CO_2 for Case 1 and reformed to H_2 and CO in Case 2 under a constant enthalpy constraint. It is shown that extinction was enhanced for both cases, but the enhancement from the plasma assisted CH_4 oxidation (Case 1) is much larger than that of CH_4 reforming. This is because when the flame was approaching extinction, the residence time was too short to complete the reactions. That is, CH_4 and its reformation products in the oxidizer stream cannot react completely to release the chemical enthalpy in the reaction zone in Case 2, but the chemical enthalpy was already released in Case 1 before reaching the reaction zone. Therefore, plasma assisted CH_4 oxidation is more effective in increasing the extinction limit than CH_4 reforming.

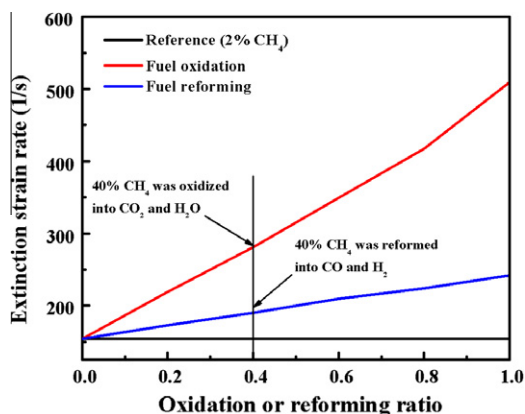


Fig. 10. Comparison of extinction strain rates of fuel oxidation and fuel reforming effect under a constant enthalpy condition for the oxidizer stream of Ar/He/ O_2/CH_4 (0.32/0.4/0.26/0.02 by volume), $P = 60$ Torr.

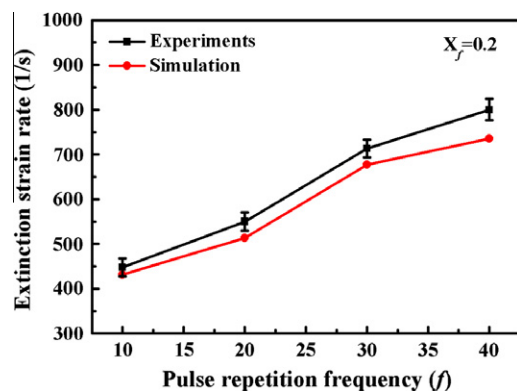


Fig. 11. Dependence of extinction strain rate on pulse repetition frequency at a fuel side CH_4 mol fraction of $X_f = 0.2$, an oxidizer side volumetric composition of Ar/He/ O_2/CH_4 (0.32/0.4/0.26/0.02), and $P = 60$ Torr.

The extinction strain rate measurements and simulations were also conducted at $f = 20, 30$ and 40 kHz (with oxidizer temperature $T_o = 743 \pm 5$ K, 843 ± 7 K and 933 ± 8 K, the oxidizer side flow rates were 1.66 SLPM, 1.89 SLPM and 1.92 SLPM, respectively, and with measured and calculated boundary conditions as described above) by fixing the fuel mole fraction and are shown in Fig. 11. With the further oxidation of CH_4 (increased f) in the partially-premixed oxidizer stream, the extinction strain rates increased significantly. With further increase of f , the experimental and simulation results deviated, which may indicate that there are additional reaction paths to enhance the flame extinction. Nonetheless, the maximum deviation was small at approximately 10%. Moreover, the peak concentration of H_2 was 1751 ppm at $f = 20$ kHz, and the extinction limit enhancement from H_2 was only 5.3%. Thus, the dominant enhancement mechanism for the extinction limit is plasma-induced prompt CH_4 oxidation.

4. Conclusion

The present experiments employing a nanosecond plasma discharge in a partially premixed counterflow flame showed that plasma assisted CH_4 oxidation at low temperature (60 Torr) can extend the extinction limits dramatically. It was found that the main cause of the combustion enhancement was due to a kinetic-thermal effect of prompt CH_4 oxidation and heat release by plasma generated species. Although plasma assisted combustion led to partial CH_4 reforming to H_2 and CO , numerical simulations showed that the effect of CH_4 reforming on combustion enhancement was mainly through the rapid H_2 chemistry but only played a minor role compared to the prompt CH_4 oxidation.

The results also showed that O production by the plasma discharge was the main contributor to the prompt CH_4 oxidation at low temperature and that partial premixing of fuel in the oxidizer stream led to a dramatic decrease of O concentration due to its rapid consumption by CH_4 oxidation. The path flux analysis showed that O was generated primarily by the discharge via direct electron impact dissociation of O_2 and O_2 collisions with electronically excited species. In addition, the results also showed that the electron impact and excited species collisional dissociation of fuel also contributed approximately a mole fraction of 0.1 of the radical production.

The extinction strain rates from experimental measurements agreed well with the numerical simulations at low pressure. Comparison of measured and predicted species concentrations in plasma assisted CH_4 oxidation showed that the low temperature plasma combustion kinetic model reasonably predicted the O and CH_2O formation, but the model over-predicted the concentrations of CO , H_2O , H_2 and under-predicted the concentration of CO_2 . In order to improve the predictability of the plasma flame kinetic model, the elementary reaction rates of O production by electron impact and excited species collision need to be revisited. In addition, more experimental validation data in flow reactors of CH_4 oxidation at temperatures between 300 K and 700 K with radical addition are necessary.

Acknowledgments

This work was supported by the MURI research grant from the Air Force Office of Scientific Research and the Grant FA9550-07-1-0136 under the technical monitor of program manager Dr. Julian Tishkoff. Wenting Sun thanks Francis Haas, Saeid Jahangirian, Joshua Heyne and Joe Lefkowitz from the Department of Mechanical and Aerospace Engineering, Princeton University for the help with the FTIR and GC measurements.

References

- [1] T. Ombrello, Y. Ju, A. Fridman, *AIAA J.* 46 (2008) 2424–2433.
- [2] T. Ombrello, X. Qin, Y. Ju, A. Gutsol, A. Fridman, C. Carter, *AIAA J.* 44 (2006) 142–150.
- [3] S.A. Bozhenkov, S.M. Starikovskaia, A.Y. Starikovskii, *Combust. Flame* 133 (2003) 133–146.
- [4] A.Y. Starikovskii, N.B. Anikin, I.N. Kosarev, E.I. Mintoussov, S.M. Starikovskaia, V.P. Zhukov, *Pure Appl. Chem.* 78 (2006) 1256–1298.
- [5] S.M. Starikovskaia, *J. Phys. D: Appl. Phys.* 39 (2006) R265–R299.
- [6] G. Lou, A. Bao, M. Nishihara, S. Keshav, Y.G. Utkin, J.W. Rich, W.R. Lempert, I.V. Adamovich, *Proc. Combust. Inst.* 31 (2007) 3327–3334.
- [7] E. Mintusov, A. Serdyuchenko, I. Choi, W.R. Lempert, I.V. Adamovich, *Proc. Combust. Inst.* 32 (2009) 3181–3188.
- [8] M. Uddi, N. Jiang, E. Mintusov, I.V. Adamovich, W.R. Lempert, *Proc. Combust. Inst.* 32 (2009) 929–936.
- [9] S.V. Pancheshnyi, D.A. Lacoste, A. Bourdon, C.O. Laux, *IEEE Trans. Plasma Sci.* 34 (2006) 2478–2487.
- [10] N. Chintala, R. Meyer, A. Hicks, A. Bao, J.W. Rich, W.R. Lempert, I.V. Adamovich, *J. Propul. Power* 21 (2005) 583–590.
- [11] I.N. Kosarev, N.L. Aleksandrov, S.V. Kindysheva, S.M. Starikovskaia, A.Y. Starikovskii, *J. Phys. D: Appl. Phys.* 41 (2008) 032002 (1–6).
- [12] A.M. Starik, V.E. Kozlov, N.S. Titova, *Combust. Flame* 157 (2010) 313–327.
- [13] W. Kim, M.G. Mungal, M.A. Cappelli, *Combust. Flame* 157 (2010) 374–383.
- [14] G. Pilla, D. Galley, D.A. Lacoste, F. Lacas, D. Veynante, C.O. Laux, *IEEE Trans. Plasma Sci.* 34 (2006) 2471–2477.
- [15] T. Ombrello, S.H. Won, Y. Ju, S. Williams, *Combust. Flame* 157 (2010) 1906–1915.
- [16] T. Ombrello, S.H. Won, Y. Ju, S. Williams, *Combust. Flame* 157 (2010) 1916–1928.
- [17] W. Sun, M. Uddi, T. Ombrello, S.H. Won, C. Carter, Y. Ju, *Proc. Combust. Inst.* 33 (2011) 3211–3218.
- [18] N.L. Aleksandrov, S.V. Kindysheva, I.N. Kosarev, S.M. Starikovskaia, A.Y. Starikovskii, *Proc. Combust. Inst.* 32 (2009) 205–212.
- [19] G.D. Stancu, F. Kaddouri, D.A. Lacoste, C.O. Laux, *J. Phys. D: Appl. Phys.* 43 (2010) 124002 (1–10).
- [20] X. Rao, K. Hemawan, I. Wichman, C. Carter, T. Grotjohn, J. Asmussen, T. Lee, *Proc. Combust. Inst.* 33 (2010) 3233–3240.
- [21] S.H. Won, M.S. Cha, C.S. Park, S.H. Chung, *Proc. Combust. Inst.* 31 (2007) 963–970.
- [22] A. Schutze, J.Y. Jeong, S.E. Babayan, J. Park, J.S. Selwyn, R.F. Hicks, *IEEE Trans. Plasma Sci.* 26 (1998) 1685–1694.
- [23] K. Niemi, V. Schulz-von der Gathen, H.F. Dobebe, *Plasma Sources Sci. Technol.* 14 (2005) 75–386.
- [24] H. Wang, X. You, A.V. Joshi, S.G. Davis, A. Laskin, F. Egolfopoulos, C.K. Law, <http://ignis.usc.edu/USC_Mech_II.htm>.
- [25] I.V. Adamovich, J.W. Rich, G.L. Nelson, *AIAA J.* 46 (2008) 2424–2433.
- [26] A. Bao, Ignition of Hydrocarbon Fuels by a Repetitively Pulsed Nanosecond Pulse Duration Plasma, Ph.D. Dissertation, Mechanical Engineering Dept., Ohio State Univ., Columbus, OH, 2008.
- [27] M. Uddi, Non-equilibrium Kinetic Studies of Repetitively Pulsed Nanosecond Discharge Plasma Assisted Combustion, Ph.D. Dissertation, Mechanical Engineering Dept., Ohio State Univ., Columbus, OH, 2008.
- [28] I.N. Kosarev, N.L. Aleksandrov, S.V. Kindysheva, S.M. Starikovskaia, A.Y. Starikovskii, *Combust. Flame* 154 (2008) 569–586.
- [29] D.S. Stafford, M.J. Kushner, *J. Appl. Phys.* 96 (2004) 2451–2465.
- [30] A. Hicks, S. Norberg, P. Shawcross, W.R. Lempert, J.W. Rich, I.V. Adamovich, *J. Phys. D: Appl. Phys.* 38 (2005) 3812–3824.
- [31] M. Tsuji, K. Kobara, H. Obase, H. Kouno, Y. Nishimura, *J. Chem. Phys.* 94 (1994) 277–282.
- [32] M.P. Burke, F.L. Dryer, Y. Ju, *Proc. Combust. Inst.* 33 (2011) 905–912.
- [33] N.A. Popov, *High Temp.* 45 (2007) 261–279.
- [34] N. Chintala, G. Lou, I.V. Adamovich, *Combust. Flame* 144 (2006) 744–756.
- [35] K. Seshadri, F.A. Williams, *Int. J. Heat Mass Transfer* 21 (1978) 251–253.
- [36] S.H. Won, W. Sun, Y. Ju, *Combust. Flame* 157 (2010) 411–420.
- [37] R.J. Kee, F.M. Rupley, J.A. Miller, M.E. Coltrin, J.F. Grcar, E. Meeks, H.K. Moffat, A.E. Lutz, G. Dixon-Lewis, M.D. Smooke, J. Warnatz, G.H. Evans, R.S. Larson, R.E. Mitchell, L.R. Petzold, W.C. Reynolds, M. Caracotsios, W.E. Stewart, P. Glarborg, C. Wang, O. Adigun, W.G. Houf, C.P. Chou, S.F. Miller, Chemkin Collection, Release 3.7.1, Reaction Design, Inc., San Diego, CA, 2003.
- [38] Y. Ju, H. Guo, K. Maruta, *J. Fluid Mech.* 23 (1997) 315–334.
- [39] X. Rao, S. Hammack, T. Lee, C. Carter, I.B. Matveev, *IEEE Trans. Plasma Sci.* 38 (2010) 3265–3271.